

Compatible Polycarbonate/Polyamide 6,6 Blends with Fibrillar Morphology

Ainhoa Granado, Jose Ignacio Eguiazábal, Jon Nazábal

Departamento de Ciencia y Tecnología de Polímeros and Instituto de Materiales Poliméricos 'POLYMAT', Facultad de Química UPV/EHU, P. Ó. Box 1072, San Sebastián 20080, Spain

Received 11 June 2010; accepted 25 September 2010

DOI 10.1002/app.33449

Published online 17 February 2011 in Wiley Online Library (wileyonlinelibrary.com).

ABSTRACT: Blends of bisphenol A polycarbonate (PC) and polyamide 6,6 (PA6,6) were prepared directly during the plasticization step of an injection molding process in an attempt to attain both (i) the reinforcement of the blends through fibrillar morphology, and (ii) an adequate compatibilization despite the short processing procedure used. Differential scanning calorimetry and dynamic-mechanical analysis indicated that the blends were made up of a PC-rich phase where some PA6,6 was present and, ruling out a possible degradation, of an almost pure PA6,6-phase. The cryogenically fractured surfaces observed by scanning electron microscopy showed both rather fine particles and larger particles with occluded subparticles. This complex morphology indicates low interphase tension and, therefore, compatibilization, which can be attributed to the presence of PA6,6 in the two phases of the blends. The values of Young's modulus, determined by means of tensile tests, were always synergistic and, in the case of the 25/75 blend, the modulus was even higher than those of any of the two pure components. It appears this could be due to both the highly fibrillar morphology of the dispersed phase, and the significant decrease observed in specific volume. The blends remained ductile throughout the full composition range, which also indicates compatibilization. © 2011 Wiley Periodicals, Inc. *J Appl Polym Sci* 121: 161–168, 2011

Key words: blends; mechanical properties; compatibilization; structure; fibrillar morphology

INTRODUCTION

Since 1960 the consumption of polymer blends has grown about 9% annually and the same trend is expected to continue.¹ This makes polymer blends one of the most attractive, studied and developed research fields in Polymer Science and Technology by offering, among others, the potential (i) to extend engineering resins performance by diluting them with low cost commodity polymers, (ii) to improve a specific property, (iii) to develop materials with a full set of desired properties, and/or (iv) to modify the material performance to meet customers specifications.

Polyamide 6,6 (PA6,6) exhibits good solvent resistance, hydrolytic stability, abrasion resistance and mechanical strength due to its highly crystalline structure. However, it shows poor dimensional stability in humid environments due to water absorp-

tion, as well as low impact resistance in typical conditions of use. Bisphenol-A polycarbonate (PC) on the other hand, is an amorphous engineering polymer with a good combination of thermal and mechanical properties, but has poor resistance to most solvents. Both PA6,6 and PC are important commercial polymers with outstanding performance in many applications. Many of their blends with several second components have been widely studied and some of them are also commercially available.² Consequently, taking into account the characteristics of each polymer, and provided that their favorable properties are maintained, it appears that they can at least partly offset each other's shortcomings.

Unfortunately, previous attempts to blend PC and polyamides (PA) have been mostly unsatisfactory due to incompatibility, which has been observed in PC/polyamide 6 (PA6) blends^{3,4} as well as in PC/amorphous polyamide (3Me6T),^{5,6} PC/polyamide 12 (PA12), and PC/polyamide 6-co-12 blends.⁷ Compatibility can be ameliorated by the addition of a third component or modification of a component of the blend. To this end, in PC/PA6 blends, bisphenol type A epoxy resin,⁸ acrylic polymers,⁹ and styrene-maleic anhydride copolymer (SMA)¹⁰ have been used. Styrene-acrylonitrile-maleic anhydride terpolymers¹¹ have been used in PC/PA6-co-12 blends, and polyalkyloxazoline^{12,13} in PC/PA6,6 blends. An

Correspondence to: J. I. Eguiazábal (josei.eguiazabal@ehu.es).

Contract grant sponsor: Basque Government; contract grant number: GIC07/48-IT-234-07.

Contract grant sponsor: University of the Basque Country.

alternative means of achieving compatibilization is through the production of chemical reactions during processing. In this way, some studies have shown that PC and PA6 may chemically react at high temperatures and long mixing times forming PC-PA6 copolymers that act as compatibilizers.^{14–19} Shear can also induce miscibility in blends of PC with several PAs.^{5–7}

It is known that the processing method and conditions determine the size, shape, and dispersion level of the dispersed phase generated during blending,²⁰ i.e., the blend morphology, which in turn is chiefly responsible for the physical properties of the blends. For instance, the development of orientated and elongated structures can improve the mechanical properties of the blends.^{19,21,22} This is because the interphase area increases and the orientation of the dispersed phase is usually high; and these two factors, in turn, should favor the role of the dispersed phase in the overall mechanical response.

While some research has already been carried out on PC/polyamide blends, the blends of PC with the PA6,6 have not yet, to our knowledge, been studied in the open literature. This is despite the clear interest that has already led to patents on both compatibilized neat PC/PA6,6 blends,^{12,13} and on blends with SEBS-g-MA as a third component.²³ In this work, we have looked into the possibility of obtaining directly injection molded PC/PA6,6 blends with fibrillar morphology, while offering at the same time adequate compatibilization despite of the short mixing time that the direct injection procedure involves. To this end, representative compositions of PC/PA6,6 blends were directly mixed by injection molding. The phase structure of the blends was characterized by means of dynamic mechanical analysis (DMA) and differential scanning calorimetry (DSC), the morphology was analyzed by scanning electron microscopy (SEM), and the mechanical properties were determined by tensile tests.

EXPERIMENTAL

The polymers used in this work were commercial products. The polyamide 6,6 (MFI = 32 g/10 min at 270°C and with 2.16 kg load) was Zytel® 101L NC010 (Dupont), and the polycarbonate (MFI = 19 g/10 min at 300°C and with 1.2 kg load) was Tarflon® IV1900R from Idemitsu Petrochemical Co. Ltd. The density of PA6,6 was 1.14 g/cm³ and that of PC, 1.20 g/cm³. Drying before processing was performed *in vacuo* at 90°C for 14 h for PA6,6 and at 120°C in an air-circulation oven for 12 h in the case of PC.

Tensile (ASTM D-638, type IV) specimens with compositions 100/0, 75/25, 50/50, 25/75, and 0/100 (by weight) were obtained by injection molding in a

Battenfeld BA 230E reciprocating screw injection molding machine. Blending was performed directly during the plasticization stage of the injection molding process, without a prior mixing step in an extruder. The screw of the injection machine had a diameter, D , of 18 mm, a L/D ratio of 17.8, compression ratio of 4 and helix angle of 17.8°. The barrel temperature was 270°C, the mold temperature 15°C, the injection speed 11.4 cm³/s, and the injection pressure 2600 bar.

The phase structure of the blends was studied by DMA analysis performed using a DMA Q-800 from TA Instruments, which provided the plots of the loss tangent ($\tan \delta$) against temperature. The scans were carried out in single cantilever mode at a heating rate of 4°C/min and a frequency of 1 Hz from –120 to 200°C. The melting behavior was studied by DSC using a Perkin–Elmer DSC-7 calorimeter calibrated with reference to an indium standard and in a nitrogen atmosphere. The samples were first heated from 30°C up to 285°C at 20°C/min, then cooled at the same rate and subsequently reheated as for the first scan. The melting temperatures (T_m) were determined from the maximum of the endotherms of the first heating scans while the crystallization temperatures (T_c) were taken at the minimum of the exotherms of the cooling scans. The crystallization and melting enthalpies (ΔH_c and ΔH_m) were determined from the areas of the corresponding peaks. The crystallinity was calculated from the melting enthalpies, using a value of 195.9 J/g as the melting heat for the 100% crystalline PA6,6.²⁴

The possible occurrence of reactions during processing was analyzed by FTIR spectroscopy (Nicolet Magna IR 560 spectrophotometer). The FTIR spectra were obtained from the surfaces of tensile specimens using an attenuated total reflectance (ATR) objective. The specific volume of the blends was determined by the displacement method in a Mirage SD-120L electronic densitometer using butyl alcohol as the immersion liquid. The estimated resolution was 0.003 cm³/g. The specific volume of the amorphous phase was obtained from the experimental density values using the following equation:

$$\frac{1}{\rho_b} = \frac{1 - X_{PA6,6}}{\rho_a} + \frac{X_{PA6,6}}{\rho_{PA6,6c}}$$

where ρ_a is the density of the amorphous phase of the blends, $X_{PA6,6}$ is the crystalline content of the blend calculated by DSC as described previously, ρ_b is the experimental density of the blends, and $\rho_{PA6,6c}$ is the density of crystalline PA6,6 (1.24 g/cm³).²⁵

The orientation of the blends was measured using a Metricon Model 2010 equipped with an infrared laser with a wavelength of 1550 nm. The samples were prepared by sectioning the central part of the

TABLE I
Glass transition, Melting, and Crystallization Temperatures of the Blends and Crystallinity of PA6,6 as a Function of Composition

PC/PA6,6	T_g PA6,6 (°C)		T_g PC (°C)		T_m (°C)	T_c (°C)	Crystallinity (%)
	DSC	DMA	DSC	DMA			
100/0	–	–	150	154			
75/25	61	62	146	152	265	227	40
50/50	58	63	146	149	266	226	42
25/75	59	65	143	146	267	223	36
0/100	62	68	–		270	229	38

injected specimens with a Leica 1600 microtome. Vicat softening points were measured using impact specimens with an ATS-Faar MP3 HDT-Vicat tester at 50°C/h and with a 1 kg load (ASTM D-1525). Melt viscosity measurements were performed at 270°C in a Gottfert Rheograph 2002 rheometer using a flat entry capillary tungsten die of 1 mm diameter and with a L/D ratio of 30.

SEM was carried out in a Hitachi S-2700 electron microscope on the core of cryogenically fractured and gold-coated tensile specimens at an accelerating voltage of 15 kV. SEM was also used to observe the dispersed PA6,6 and PC phases after elimination of the corresponding PC and PA6,6 matrices by immersing the central part of the injection molded specimens for 36 h in 1,1,2,2-tetrachloroethane and formic acid, respectively.

Tensile testing was carried out by using an Instron 5569 machine, at a crosshead speed of 10 mm/min and at $23 \pm 2^\circ\text{C}$ and $50 \pm 5\%$ relative humidity. The mechanical properties (yield and break stresses and ductility, measured as the break strain) were determined from the load-displacement curves. Young's modulus was determined by means of an extensometer at a crosshead speed of 1 mm/min. A minimum of eight tensile specimens were tested for each reported value.

RESULTS AND DISCUSSION

Phase behavior

Table I shows the T_g 's of the blends and of the neat PC and PA6,6 as a reference, measured by both DSC and DMA. As can be seen, two T_g 's were observed whatever the blend composition, clearly indicating the presence of two amorphous phases. The high temperature T_g which corresponds to a PC-rich phase, decreased slightly but steadily both by DSC and DMA (maximum decrease 7–8°C) as the PA6,6 content of the blends increased. This indicates slight miscibilization of PA6,6 in the PC phase.^{20,26} Taking into account the very short processing time used, the presence of any reacted copolymer should be negligible. The degradation of PC during blending would

also lead to a T_g decrease. However, unlike the PC/PA6 blends of reference³, the blends in this work were molded directly without any previous extrusion. Consequently, the residence time in the melt state and the possibility for PC degradation are clearly reduced. Therefore, we propose that the T_g decrease is due to the presence of a slight amount of PA6,6 in the PC-rich phase. This amount (calculated from the Fox equation²⁷ and the experimental T_g values) was maximum (approximately 8%) in the 25/75 blend. The presence of PA6,6 in the two amorphous phases of the blends points to the processing procedure being effective enough to compatibilize the blends.

To find out whether the PA6,6 in the PC-rich phase was either mixed or reacted, FTIR analysis was conducted in the 25/75 blend, i.e., in the composition where the biggest change in high temperature T_g occurred. When the experimental and the theoretical spectra obtained from the spectra of the two components were compared (Fig. 1), no evident change was detected. This indicates that the PA6,6 is basically dissolved in the PC-rich phase. This agrees with the fast and single mixing procedure used.

The low temperature T_g of the blends, which corresponds to the PA6,6 phase, remained almost

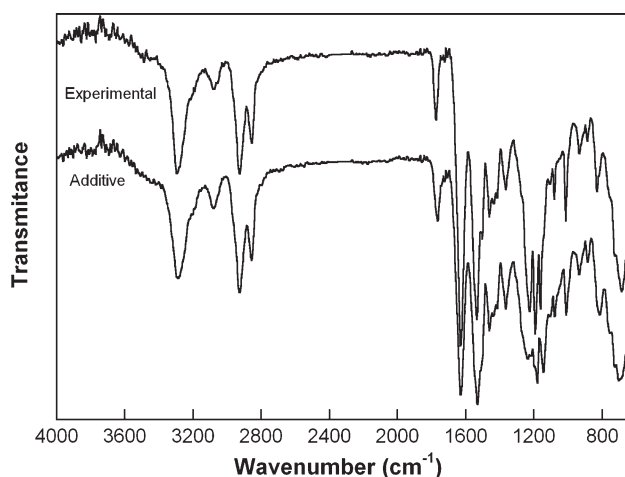


Figure 1 Experimental and calculated FTIR spectra for the PC/PA6,6 25/75 composition.

constant on the DSC scans, but decreased steadily (maximum: 6°C) by DMA at increasing PC contents. Both similar decreases²⁶ as well as no change^{3,20} have been recorded for other PC/polyamide blends. A different expansion coefficient of the blend components was proposed as the reason for a similar decrease.^{28,29} However, this effect has to take place only when one of the components is the matrix, and in our blends it occurs both in a PC and in a PA6,6 matrix. As degradation of PC can be ruled out in this study because of the short blending time used, the most plausible explanation is a selective migration of a low molecular component present in the PC (PC oligomers or an additive for instance) to the PA6,6-rich phase.

With respect to the PA6,6 crystalline phase, its amount was unaffected by the PC content of the blends (Table I). Its perfection only slightly decreased in the presence of PC, because the melting temperature in the first scan only slightly decreased (5°C in the 75/25 composition). Finally, the crystallization temperature from the melt also showed very slight changes with composition. This crystallization-melting behavior is consistent with the presence of an almost pure PA6,6 phase in the blends.

Morphology

The morphology of the blends was first studied by SEM on cryogenically fractured tensile specimens (Fig. 2). Biphasic morphology was observed whatever the composition. Many dispersed particles in the 75/25 and 25/75 blends were small (between 1 and 2 μm). This particle size is similar to that of PC/PA6 blends (1–2.5 μm) obtained either after a two-step molding procedure^{8,18} or long (15 min) mixing times.^{4,18} As can also be seen, most of the dispersed particles in the 50/50 blend contained inclusions of an obvious matrix nature. The fine particle size and the presence of inclusions indicate (i) that the direct injection molding procedure used was effective enough to properly mix the blends and (ii) that there was low interfacial tension between the components of the blend. The latter is probably a consequence of the presence of PA6,6 in the two phases of the blends as observed in the previous section, and should contribute to a high adhesion level in the solid state. This occurs despite the short mixing time that the direct injection molding procedure, which is in theory less likely to cause compatibilization, involves, and indicates that it is effective enough to compatibilize the PC/PA6,6 blends under the mixing conditions of this work.

The 50/50 blend showed a quasi cocontinuous morphology that indicated the proximity of the phase inversion region. To find out where it took place and the nature of the matrix in Figure 2(b), the

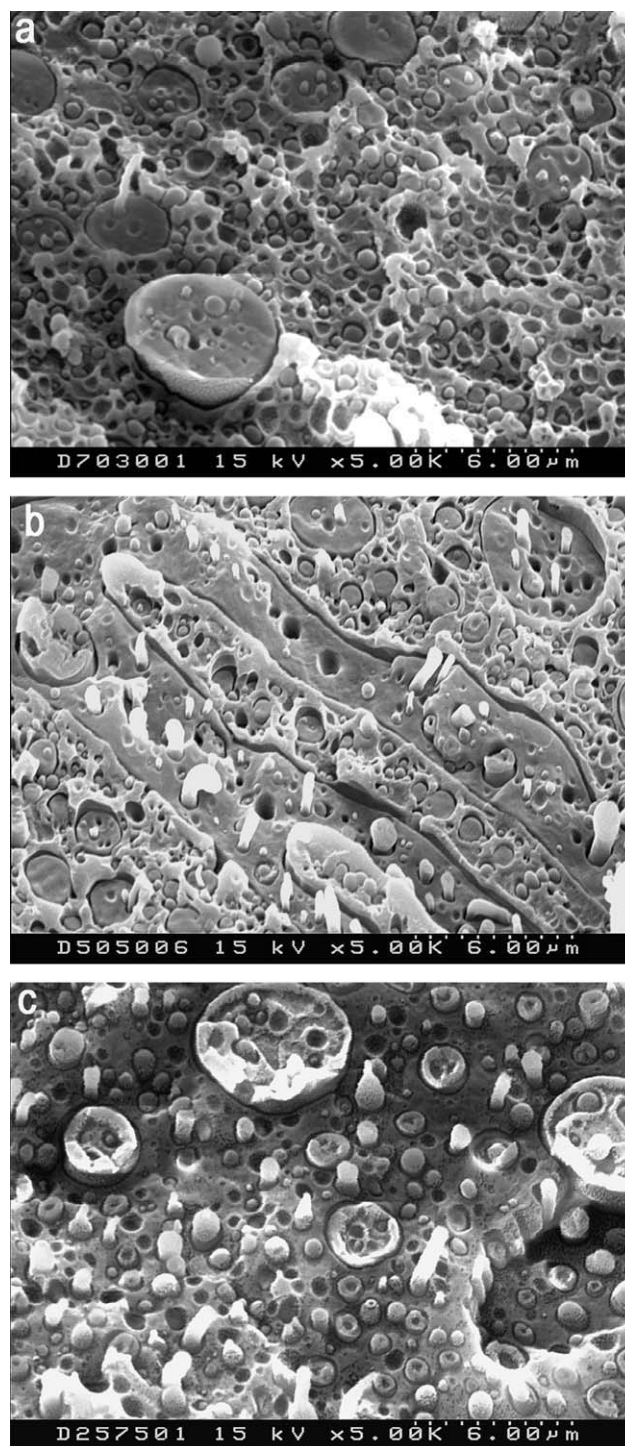


Figure 2 SEM photomicrographs of the surfaces of cryogenically fractured PC/PA6,6 75/25 (a), 50/50 (b) and 25/75 (c) blends. The photographs were obtained by SEM at an angle of 30° from the perpendicular to the surfaces.

Vicat softening temperature-composition plot is shown in Figure 3. It has been shown^{30,31} that the inflection point of the Vicat softening temperature plot against composition gives an estimation of the phase inversion composition for biphasic blends. As can be seen, the Vicat temperature of the 50/50

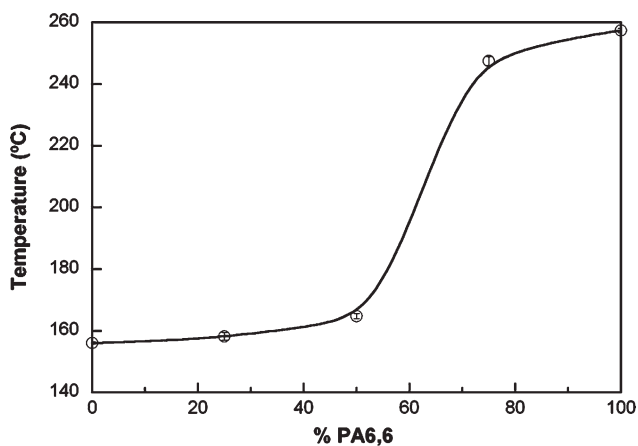


Figure 3 Vicat softening temperature of PC/PA6,6 blends as a function of composition.

blend was very close to that of PC indicating that the matrix of the 50/50 composition and the inclusions of the large dispersed phase had a PC-rich nature. Consequently, the large dispersed phases had an obvious PA6,6-rich nature.

If we observe Figure 2(c), some elongated particles appear; some fibrils were also seen in the fractured tensile specimens. Therefore, to find out to what extent the dispersed phases were fibrillar, the matrices of the 75/25 and 25/75 specimens were dissolved (see experimental section) and the morphology of the dispersed phases is shown in Figure 4(a) (PA6,6) and 4(b) (PC). As can be seen, fibrillation occurred during processing, because both dispersed phases are present as very highly fibrillated structures. To find out the reasons for the occurrence of these morphologies, it is known that^{32–35} injection molding may favor fibrillar morphology in immiscible blends under appropriate conditions. This clearly occurred not only in the case of PA6,6, which is rather prone to fibrillation when it is a dispersed phase,^{26,36} but also in the case of the PC dispersed phase which is, in theory, less prone to fibrillation.

As can also be seen in Figure 4(a), the PA6,6 was visibly more fibrillated than the PC of Figure 4(b) because the fibers were clearly thinner. It is known that in immiscible thermoplastic blends,³⁷ fibril morphologies are more easily produced (provided processing conditions and composition are the same³⁸) when the viscosity ratio ($\lambda = \eta_d/\eta_m$ where η_d and η_m are respectively, the viscosities of the dispersed phase and of the matrix) of the blends components³⁹ is below unity (the matrix more viscous than the dispersed phase). Therefore, the viscosity of the blend components was measured by capillary rheometry at a temperature of 270°C and a shear rate of 2000 s⁻¹, similar to that common in injection molding. At these conditions, the PC was more viscous (368 Pa.s) than the PA6,6 (76 Pa.s). Therefore λ is below unity when PC is the matrix and PA6,6 the dispersed

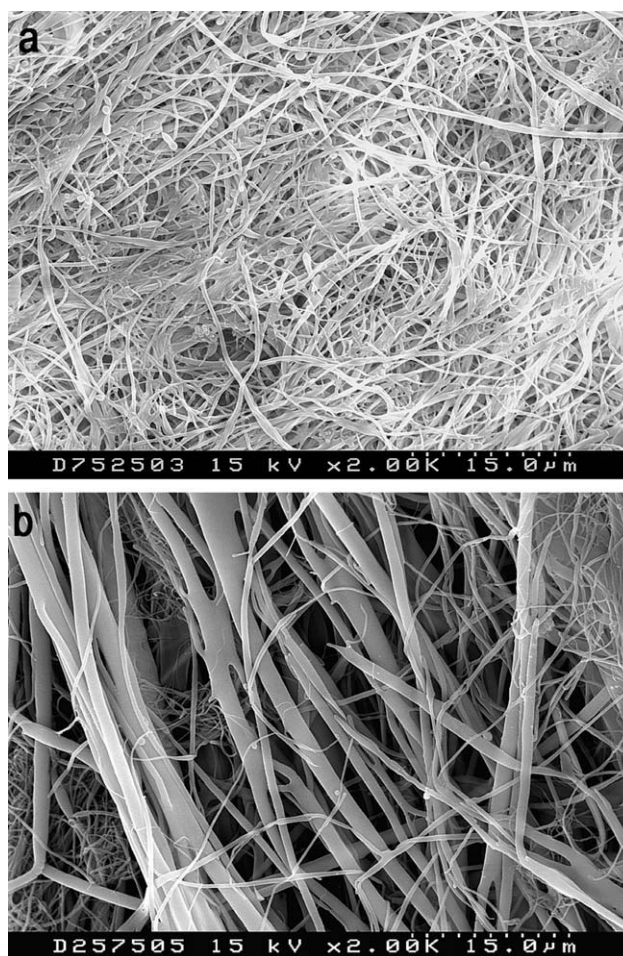


Figure 4 SEM photomicrographs of the dispersed phases of PC/PA6,6 75/25 (a) and 25/75 (b) after extraction of the corresponding matrices.

phase, in agreement with the more effective fibrillation of PA6,6 in Figure 4(a).

Mechanical properties

Young's modulus and the yield stress of the blends as a function of composition are shown in Figure 5.

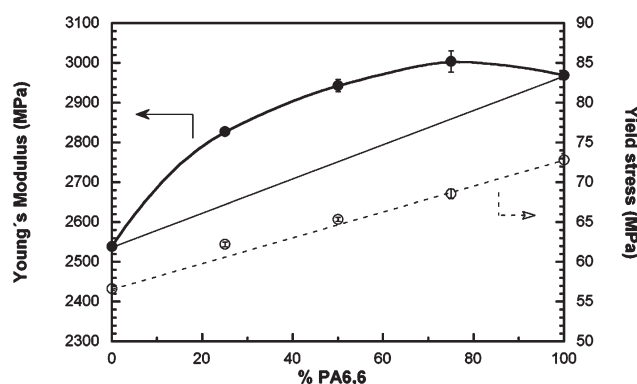


Figure 5 Young's modulus (●) and yield stress (○) of PC/PA6,6 blends as a function of composition.

As can be seen in this figure, all compositions showed modulus values higher than the linear interpolation between the values of the neat polymers. The maximum positive deviation was approximately 7%. This indicates that the modulus of the blends behaves in a synergistic way; this synergism is even absolute in the case of the 25/75 blend, as its modulus is slightly higher than that of any of the two pure components. The behavior of the yield stress was almost linear, because the observed deviations were comparable with the standard deviation of the values. This is to be expected, because in polymer blends the deviations in the yield stress are usually^{40,41} smaller than those of the elastic modulus.

It is known that morphological effects such as orientation, free volume changes, or modified crystallization can lead to synergistic modulus behavior in immiscible polymer blends.^{20,42,43} For instance, in PC/PA6 blends with a globular morphology negative¹⁸ or lineal²⁰ modulus were observed, while modulus increases of 12% were obtained when fibers were present.²⁰ Therefore, to explain the synergistic behavior of the modulus of elasticity, the crystallinity of PA6,6, the free volume of the amorphous phase of the blends and the orientation of the blends were measured and compared with those of the neat components. The crystallinity of PA6,6 was hardly affected by changes in the blend composition (Table I), so it did not influence the modulus behavior. The specific volume of the blends and that calculated for the amorphous phase (see experimental section) are shown in Figure 6. As observed, there is a densification in the blends (specific volume decrease) that reaches $0.01 \text{ cm}^3/\text{g}$ in the 25/75 composition. This decrease is significant, occurs as the modulus increases in all the compositions, and has led to clear modulus increases in other blends.^{42,44–46}

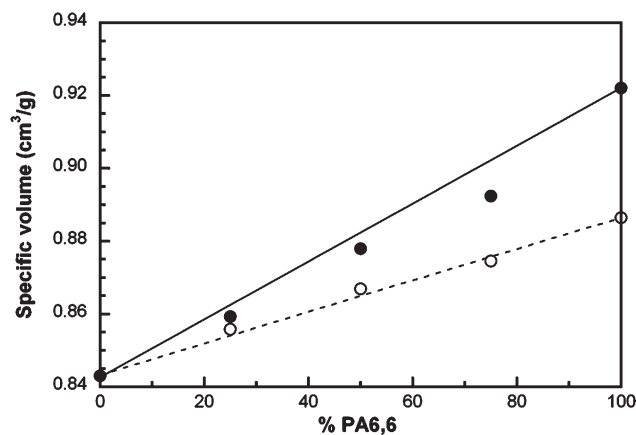


Figure 6 Specific volume (○) and specific volume of the amorphous phase (●) of PC/PA6,6 blends as a function of composition. The standard deviation of the measurement is smaller than the symbols.

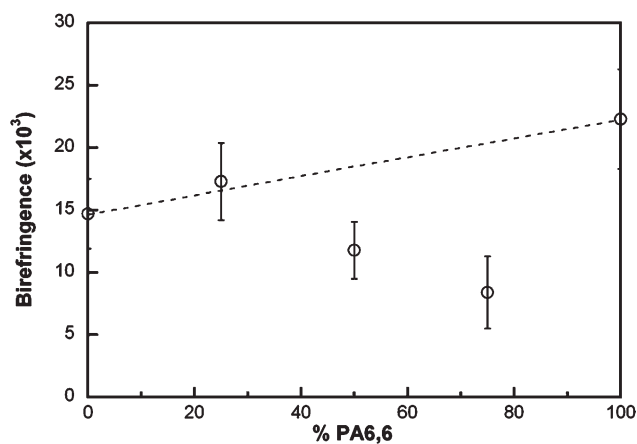


Figure 7 Birefringence of PC/PA6,6 blends as a function of composition.

The orientation of the blends was studied by means of birefringence measurements and the results are shown in Figure 7. As can be seen, with the exception of the 75/25 composition, the birefringence and consequently the matrix orientation, was smaller in the blends than in the neat components. However, as seen in the previous section, the morphology of the blends was fibrillar and consequently orientated: this indicates that the orientation throughout the specimens was not uniform and that the dispersed phase was clearly more orientated than the matrix. As the more fibrillated structures (that must reinforce the blends more effectively) developed at high PC contents, we can conclude that, while blend densification also plays a role, fibrillation is probably mostly responsible for the synergistic modulus behavior of PC/PA6,6 blends.

The ductility of the blends measured by the elongation at break is shown in Figure 8 versus the PA6,6 content. The break stress showed an analogous trend characterized by both a negative

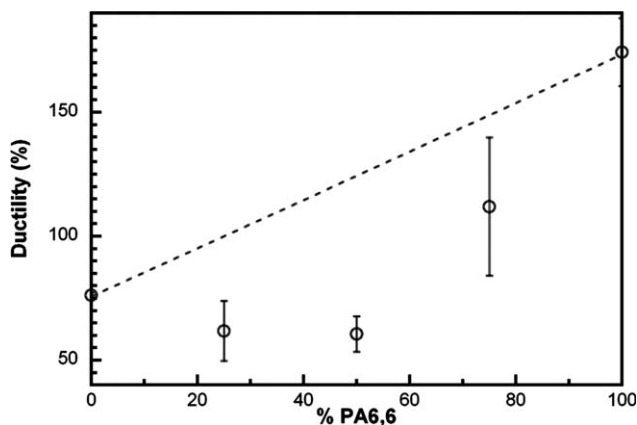


Figure 8 Ductility, measured as elongation at break, of PC/PA6,6 blends as a function of composition.

deviation with respect to linearity and a minimum value at the 50/50 composition. All the blends presented high ductility values taking into account their biphasic nature. The favorable mechanical behavior of Figure 8 appears despite the biphasic nature of the blends, and indicates that the interfacial adhesion is, in agreement with the morphology results, high enough to transmit the stress from the matrix to the dispersed phase. When the parameters that affected the ductility of the blends were determined, the crystallinity of PA6,6 did not change. The densification of the amorphous phase should lead to a negative deviation from linearity. The ductility values should be affected positively by the high interfacial adhesion previously commented in the morphology section. In addition, the importance of fibrillar morphology on ductility has been demonstrated in PC/PA6 blends,²⁰ where fibrillar morphology led to ductile blends, while globular morphology led to a brittle^{8,20} behavior. Therefore, the ductile behavior of the PC/PA6,6 blends in this study is attributed to both the compatibilizing effect of the PA6,6 mixed in the PC-rich phase, and to the presence of fibrillar morphology.

CONCLUSIONS

PC/PA6,6 blends obtained by direct injection molding are composed of an almost pure PA6,6 phase and a PC-rich phase where some PA6,6 is dissolved. No reaction was observed, probably due to the short processing time used. Neither the PA6,6 crystalline content, nor the perfection of the crystalline phase changed upon blending.

The cryogenically fractured surfaces showed the presence of a small dispersed particle size, which, together with the subparticles inside the larger dispersed phases, indicates low interfacial tension on the one hand and compatibilization on the other. Fibrillation of the dispersed phases occurred during processing regardless of the composition, and was more apparent in the PA6,6 than in the PC.

Young's modulus behavior was synergistic, being even absolute in the case of the 25/75 blend. This is attributed to densification and mainly to the orientation of the dispersed phase. The ductile nature of the blends is attributed to both the compatibilizing activity of the PA6,6 mixed in the PC-rich phase which appears despite the short processing time used, and also to the presence of fibril morphologies. Thus, to conclude, despite the short duration of this direct injection molding mixing procedure, it is long enough to enable effective blending and compatibilization of the blends and in addition, it results in favorable fibrillar morphology of the dispersed phases.

References

1. www.plasticseurope.org.
2. Utracki, L. A. *Commercial Polymer Blends*; Chapman & Hall: London, 1998.
3. Gattiglia, E.; Turturro, A.; Pedemonte, E. *J Appl Polym Sci* 1989, 38, 1807.
4. Gattiglia, E.; Turturro, A.; Pedemonte, E.; Dondero, G. *J Appl Polym Sci* 1990, 41, 1411.
5. Kim, Y. H.; Akiyama, S. *Polym Networks Blends* 1997, 7, 93.
6. Kim, Y. H.; Akiyama, S. *Polym J* 1997, 29, 296.
7. Kim, Y. H.; Akiyama, S. *Polym J* 1997, 29, 592.
8. Tjong, S. C.; Meng, Y. Z. *Mater Res Bull* 2004, 39, 1791.
9. Arjunan, P.; Mininni, R. M.; Sangani, H.; Natarajan, K. M. *Polym Mater Sci Eng* 1996, 75, 285.
10. Choi, H. K.; Cha, Y. J.; Lee, Y. M.; Kitano, T.; Horiuchi, S. *Korean Polym J* 1996, 4, 45.
11. Kim, Y. H.; Kikuchi, M.; Akiyama, S.; Sho, K.; Izawa, S. *Polymer* 1999, 40, 5273.
12. Bruce, P. T.; Bruce, A. K. U.S. Pat. 4,954,579 (1990).
13. Bruce, P. T. U.S. Pat. 4,883,836 (1989).
14. Eguiazabal, J. I.; Nazabal, J. *Makromol Chem Macromol Symp* 1988, 20/21, 255.
15. Cortázar, M.; Eguiazabal, J. I.; Iruin, J. J. *Br Polym J* 1989, 21, 395.
16. Costa, D. A.; Oliveira, C. M. F. *J Appl Polym Sci* 1998, 69, 857.
17. Valenza, A.; La Mantia, F. P.; Gattiglia, E.; Turturro, A. *Int Polym Process* 1994, 9, 240.
18. Gattiglia, E.; Turturro, A.; La Mantia, F. P.; Valenza, A. *J Appl Polym Sci* 1992, 46, 1887.
19. Gattiglia, E.; La Mantia, F. P.; Turturro, A.; Valenza, A. *Polym Bull* 1989, 21, 47.
20. Eguiazabal, J. I.; Nazabal, J. *Plast Rubber Compos Process Appl* 1990, 14, 211.
21. Cui, L.; Bara, J. E.; Brun, Y.; Yoo, Y.; Yoon, P. J.; Paul, D. R. *Polymer* 2009, 50, 2492.
22. Maxwell, B.; Jasso, G. L. *Polym Eng Sci* 1983, 23, 614.
23. Easteal, A. J.; Liao, C. W. O. Pat. 02/00793 (2002).
24. Chavarria, F.; Paul, D. R. *Polymer* 2004, 45, 8501.
25. Brandrup, J.; Immergut, E. H.; Grulke, E. A. *Polymer Handbook*; Wiley: New Jersey, 1999.
26. Goitisoló, I.; Eguiazabal, J. I.; Nazabal, J. *Eur Polym J* 2008, 44, 1978.
27. Fox, T. G. *Bull Am Phys Soc* 1956, 1, 123.
28. Kim, W. N.; Park, C. E.; Burns, C. M. *J Appl Polym Sci* 1993, 49, 1003.
29. Lee, S. G.; Lee, J. H.; Choi, K. Y.; Rhee, J. M. *Polym Bull* 1998, 40, 765.
30. Bastida, S.; Eguiazabal, J. I.; Nazabal, J. *Polym Test* 1993, 12, 233.
31. Guerrica-Echevarría, G.; Eguiazabal, J. I.; Nazabal, J. *J Appl Polym Sci* 1999, 72, 1113.
32. Li, X.; Chen, M.; Huang, Y. *Polym J* 1997, 29, 975.
33. Li, Z. M.; Yang, W.; Yang, S.; Huang, R.; Yang, M. B. *J Mater Sci* 2004, 39, 413.
34. Li, Z. M.; Xie, B. H.; Yang, S.; Huang, R.; Yang, M. B. *J Mater Sci* 2004, 39, 433.
35. Li, Z. M.; Qian, Z. Q.; Yang, M. B.; Yang, W.; Xie, B. H.; Huang, R. *Polymer* 2005, 46, 10466.
36. Olabisi, O. *Handbook of Thermoplastics*; Marcel Dekker: New York, 1997.
37. Xu, H. S.; Li, Z. M.; Pan, J. L.; Yang, M. B.; Huang, R. *Macromol Mater Eng* 2004, 289, 1087.
38. Ruiz de Gauna, B. E.; Gaztelumendi, M.; Nazabal, J. *Polym Compos* 1999, 20, 553.
39. Yi, X. S. *Handbook of Engineering Polymeric Materials*; Marcel Dekker Inc.: New York, 1997.
40. Marcus, D. Z.; Simon, G. P.; Tant, M. R.; Small, J. D.; Stack, G. M.; Hill, A. *J Polym Int* 1995, 36, 127.

41. Granado, A.; Eguiazábal, J. I.; Nazábal, J. *Macromol Mater Eng* 2004, 289, 281.
42. Ramiro, J.; Eguiazábal, J. I.; Nazábal, J. *Polym Adv Tech* 2003, 14, 129.
43. García, M.; Eguiazábal, J. I.; Nazábal, J. *Polym Eng Sci* 2002, 42, 413.
44. Vallejo, J.; Eguiazábal, J. I.; Nazábal, J. *J Appl Polym Sci* 2001, 80, 885.
45. Rodríguez, J. L.; Eguiazábal, J. I.; Nazábal, J. *J Macromol Sci Phys* 1997, 36, 773.
46. Gaztelumendi, M.; Nazábal, J. *Polym Eng Sci* 2000, 40, 430.